Food Chemistry: X 23 (2024) 101632

Contents lists available at ScienceDirect

Food Chemistry: X

journal homepage: www.sciencedirect.com/journal/food-chemistry-x

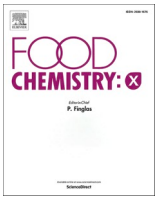

Effect of glycation with three polysaccharides on the structural and emulsifying properties of ovalbumin

Yaxue Hu [a,b], Qiqi Bian [a,b], Lijia Chen [a,b], Xichang Wang [b], Jian Zhong [a,b,c,d,*]

[a] Medical Food Laboratory, Shanghai Key Laboratory of Pediatric Gastroenterology and Nutrition, Shanghai Institute for Pediatric Research, Xinhua Hospital, Shanghai Jiao Tong University School of Medicine, Shanghai 200092, China
[b] National R&D Branch Center for Freshwater Aquatic Products Processing Technology (Shanghai), Integrated Scientific Research Base on Comprehensive Utilization Technology for By-Products of Aquatic Product Processing, Ministry of Agriculture and Rural Affairs of the People's Republic of China, Shanghai Engineering Research Center of Aquatic-Product Processing and Preservation, College of Food Science & Technology, Shanghai Ocean University, Shanghai 201306, China
[c] Department of Clinical Nutrition, College of Health Science and Technology, Shanghai Jiao Tong University School of Medicine, Shanghai 200135, China
[d] Marine Biomedical Science and Technology Innovation Platform of Lingang Special Area, Shanghai 201306, China

ARTICLE INFO

Keywords:
Creaming stability
Fish oil
Xanthan gum
Guar gum
Konjac glucomannan

ABSTRACT

Herein, three types of ovalbumin (OA)-polysaccharide conjugates were prepared with three polysaccharides (XG: xanthan gum; GG: guar gum; KGM: konjac glucomannan) for the fish oil emulsion stabilization. The glycation did not change the spectra bands and secondary structure percentages of OA, whereas it decreased the molecular surface hydrophobicity of OA. The initial emulsion droplet sizes were dependent on the polysaccharide types, OA preparation concentrations, polysaccharide: OA mass ratios, and glycation pH. The emulsion stability was mainly dependent on the polysaccharide types, polysaccharide: OA mass ratios, and glycation pH. However, it was minorly dependent on the OA preparation concentrations. The emulsions stabilized by conjugates with high polysaccharide: OA mass ratios (e.g., ≥3:5 for OA-GG) or appropriate glycation pH (e.g., 5.0–6.1 for OA-XG) showed no obvious creaming during the room temperature storage. This work provided basic knowledge on the structural modification and functional application of a protein.

1. Introduction

Ovalbumin (OA) is the major protein in egg white (≈54% by weight) and has a molecular weight of 45 kDa with 386 amino acids. Besides its significant nutritional values, it has excellent functional properties such as gelling, foaming, and emulsifying properties (Chen et al., 2024). Therefore, OA is an outstanding food hydrocolloid and has been widely applied as gelling, foaming, and emulsifying agents in the food processing field (Rostamabadi et al., 2023). It is also a promising ingredient to prepare delivery vehicles for functional foods and pharmaceuticals (Zeng et al., 2022).

The emulsifying properties of OA are subjected to variations in food matrix and processing conditions. Typical food matrix factors include oil concentrations (Mine et al., 1991), interfacial film types (e.g., Tween addition) (Li, Xue, et al., 2022), etc. Typical processing conditions include pH, ionic strength, heat, high pressure, etc. (Galazka et al., 2000). OA is in a sphere shape as a Pickering emulsifier at pH 3 and in a polymeric shape as a traditional emulsifier at pH 7 (Xu et al., 2020). Molecular modification such as glycation could improve the structure and functional behaviors of OA (Yang, Wang, et al., 2022). Therefore, it is important to explore novel modification methods to tackle these bottlenecks for the wider application of OA in the food field.

Many molecular modification methods have been developed to improve the emulsifying properties of OA. Phosphorylation could increase the emulsifying properties of OA by inhibiting protein aggregation to cause more protein adsorption on the oil/water interface (Tang et al., 2019). Hydroxyl radical-induced oxidation could improve the emulsifying properties of OA by changing the surface chemical groups and structures (Li et al., 2019). The physical and oxidative stability of the emulsions stabilized by OA could be improved by procyanidins mixing (Wen et al., 2022). The synergistic modification of enzymatic hydrolysis and phosphorylation induced better emulsifying properties than both the hydrolyzed and unmodified OAs (Liu et al., 2020). Polysaccharide xanthan gum (XG) addition could promote the emulsifying

* Corresponding author at: Medical Food Laboratory, Shanghai Key Laboratory of Pediatric Gastroenterology and Nutrition, Shanghai Institute for Pediatric Research, Xinhua Hospital, Shanghai Jiao Tong University School of Medicine, Shanghai 200092, China.
E-mail address: jzhong@shsmu.edu.cn (J. Zhong).

https://doi.org/10.1016/j.fochx.2024.101632
Received 14 January 2024; Received in revised form 2 July 2024; Accepted 5 July 2024
Available online 6 July 2024

properties of OA to stabilize soybean oil emulsions (Xiao et al., 2021). The electrostatic complexation between polysaccharide gum Arabic and OA induced higher emulsion stabilization ability than OA (Li, Zhang, et al., 2022). Controlled glycation with neutral dextran could improve the emulsifying properties of OV (Zheng et al., 2022). These works significantly promoted the development and application of OA-based food emulsifiers in the field of food science. Especially, polysaccharide glycation of protein is a mature method to prepare protein-polysaccharide conjugates with improved functional properties (Zhang et al., 2021). However, the effect of polysaccharide glycation on the structural and emulsifying properties of OA has not been systematically studied until now.

Non-gelling food polysaccharides are a class of polysaccharides that remain fluid or viscous solutions when they are completely hydrated or dispersed in water (Yang, Li, Li, Sun, & Guo, 2020). They are commonly used as thickening agents, dispersing agents, and emulsifying agents in the food industry. Typical non-gelling food polysaccharides include anionic XG, nonionic guar gum (GG), and nonionic konjac glucomannan (KGM). Anionic XG has a D-glucose backbone with some trisaccharide side chains in the molecular chain (Nsengiyumva et al., 2024). Nonionic GG has a mannose backbone with some galactose side chains in the molecular chain (Sharma et al., 2018). Nonionic KGM has β-1,4-linked mannose and glucose units in the molecular chain (Li, Wang, et al., 2022). It is well known KGM can self-associate to form a thermally irreversible gel network in the alkali environments (Yang, Li, Li, Li, et al., 2020). Therefore, XG, GG, and KGM were commonly chosen as representative food polysaccharides to improve the properties of food polymers (Lan & Lai, 2023).

The purpose of this work was to study the effect of glycation with three polysaccharides (XG, GG, and KGM) on the structural and emulsifying properties of OA. First, three types of OA-polysaccharide conjugates (OPCs) were prepared according to a glycation protocol and confirmed by observation and the analyses of the degrees of grafting (DGs). Second, the structural properties of OPCs were determined using scanning electron microscopy (SEM), attenuated total reflectance Fourier transform infrared (ATR-FTIR) spectrometry, secondary structure percentage analyses, and molecular surface hydrophobicity analyses. Third, the effects of OA preparation concentrations and polysaccharide types on the preparation and stability of the OPC-stabilized emulsions were studied using digital camera technique and optical microscopy. Fourth, the effect of the GG: OA mass ratio on the preparation and stability of the OPC-stabilized emulsions was investigated using digital camera technique and optical microscopy. Fifth, the effect of glycation pH on the preparation and stability of the OPC-stabilized emulsions was analyzed using digital camera technique and optical microscopy.

2. Materials and methods

2.1. Materials

XG (USP grade, CAS No.: 11138–66-2, Production No.: GB810381; Ash content: 11.7%; Loss on drying: 10.3%; Heavy metals: 13.8 ppm) and OA (BR grade, CAS No.: 9006-59-1, Production No.: E6337, Water: 0%–10%, Molecular weight: 44–45 kDa) was purchased from Shanghai Macklin Biochemical Co., Ltd., China. GG (AR grade, CAS No.: 9000-30-0, Production No.: S30550, Solubility: 10 mg/mL in water), and KGM (Viscosity ≥15,000 mpa.s, CAS No.: 37220–17-0, Production No.: S30903, Solubility: 40 mg/mL in water) were purchased from Shanghai Yuanye Biotechnology Co., Ltd., China. Fish oil (DHA + EPA ≥ 70%) was bought from Xi'an Qianyecao Biological Technology Co., Ltd., Shaanxi, China. The other common materials were bought from Sinopharm Chemical Reagent, Shanghai, China.

2.2. Preparations of OPCs

The OPCs were fabricated using a glycation protocol in our and others' previous work (Hu et al., 2022; Huang et al., 2020; Zhang et al., 2022). Basic experimental process was described as below: solid polysaccharide reagents (XG, GG, and KGM) were mixed with 5 mL of OA (Shanghai Aladdin) solution (10 mg/mL). Then, 0.01 g of polysaccharide was added to the solution. The pH was pH 6.1. Then, the mixtures were Vortexed for 30 s and were incubated at 90 °C for 1 h to obtain OPC solutions. The OPC solutions were freeze-dried to obtain solid OPC samples. The protein-polysaccharide conjugates and raw materials (protein and polysaccharide) were macromolecules. Therefore, almost all the works on the development and application of protein-polysaccharide conjugates did not separate the protein-polysaccharide conjugates from the raw materials (protein and polysaccharide) after the glycation (Amiratashani et al., 2024; Feng et al., 2023).

Different OA concentration (2, 4, 6, 10, and 15 mg/mL; polysaccharide concentration of 2 mg/mL, unchanged pH), polysaccharide: OA mass ratios (1:5, 2:5, 3:5, 4:5, and 1:1; OA concentration of 10 mg/mL; unchanged pH), and glycation pH (3.0, 5.0, 7.0, 9.0, and 11.0; OA concentration of 10 mg/mL, polysaccharide concentration of 2 mg/mL) were explored to analyze their effects on the structural and emulsifying properties of OPCs. The pH was adjusted with 1 mol/L of HCl and 1 mol/L of NaOH. The untreated OA solutions were stored at room temperature to show their solubilization in water.

2.3. Degree of grafting

The DGs were obtained using a typical *O*-phthalaldehyde (OPA) method (Wen et al., 2020). Briefly, 50 mL of OPA reagent was freshly prepared by mixing 1 mL of 40 mg/mL OPA methanol solution, 2.5 mL of 20% (*w*/w) sodium dodecyl sulfate solution, 25 mL of 0.1 mol/L sodium tetraborate buffer, 100 μL of β-mercaptoethanol, and water. Then, 4 mL of OPA reagent was mixed with 200 μL of OPC solution. The mixture was incubated in the dark for 2 min at 35 °C. Subsequently, the mixture absorbance was determined at 340 nm using a Persee T6 UV–Vis spectrophotometer (Beijing, China). A mixture of 4 mL OPA reagent with 200 μL of water was used as the reference solution. DG (%) was calculated by dividing the absorbance differences between the OA/polysaccharide mixture and OPC solution by the absorbance of the OA/polysaccharide mixture and multiplying by 100.

2.4. Scanning electron microscopy

The freeze-dried OPC samples were attached to a conductive adhesive, sputtered for 90 s, and examined using Hitachi SU5000 scanning electron microscope (Japan) with a voltage of 5.0 kV. The OA or polysaccharides without each other were treated with the same OPC preparation procedure and then observed by SEM.

2.5. ATR-FTIR spectroscopy and secondary structure analysis

The freeze-dried OPC samples were examined using a PerkinElmer Spotlight 400 ATR-FTIR spectrometer (Waltham, MA, USA) with a spectra range of 600–4000 cm^{-1} (Hu et al., 2022). The scan resolution was 1 cm^{-1}. The spectra (1700–1600 cm^{-1}) were analyzed using SeaSolve PeakFit software (V4.12, San Jose, CA, USA) to obtain the secondary structure percentages. The OA or polysaccharides without each other were treated with the same OPC preparation procedure and then analyzed by ATR-FTIR spectrometry as controls.

2.6. Molecular surface hydrophobicity

Molecular surface hydrophobicity of OPCs and OA were measured using a 1-anilino-8-naphthalenesulfonate magnesium salt (ANS)

fluorescent probe method (Xu et al., 2022). OPCs and OA were dissolved in phosphate buffer solution (0.05 mol/L, pH 7.0) at a concentration of 1.0 mg/mL. Then, the solutions were diluted to 0.2–1.0 mg/mL. Then, 15 μL of ANS phosphate buffer solution (0.05 mmol/L) was mixed with 6 mL of the sample solution. After 30 min in the dark, the fluorescence intensity of the samples was determined using an F-7000 fluorescence spectrophotometer (Hitachi, Tokyo, Japan) with an excitation wavelength of 390 nm and an emission wavelength of 470 nm. The fluorescence intensity versus protein concentration (g/L) was plotted and fitted by a linear equation. The slope was the molecular surface hydrophobicity of OPCs or OA.

2.7. OPC-stabilized fish oil emulsions

The emulsions were prepared using a homogenizer (T10, IKA, Guangzhou City, Guangdong Province, China) (Hu et al., 2022). Briefly, 5 mL of the OPC solution was mixed with 5 mL of fish oil (Xi'an Qianyecao, Shaanxi, China). The mixture was treated with the homogenizer for 90 s at a speed of 11,500 rpm. The emulsions were stored at room temperature.

The emulsions were photographed using a digital camera. The emulsion creaming index (CI) value (%) was dividing the serum layer height by the emulsion height and multiplying by 100. The emulsions were observed using an upright optical microscope (ML8000, Shanghai Minz, China) with an objective of 40×. Optical images were randomly chosen from three independent experiments (≥ one from each) and all the droplet sizes in these images were fully measured using the commercial microscope software. The sizes (500–700 values) were analyzed by the frequency distribution and multiple peak Gaussian fitting.

2.8. Statistical analysis

Mean ± standard deviation was used to express the obtained data ($n = 3$). One-way ANOVA with Duncan's analysis was used for the statistical analysis.

3. Results and discussion

3.1. Preparation and confirmation of OPCs

Protein glycation is the initial stage of the Maillard reaction process between proteins and polysaccharides, which generally includes the initial, intermediate, and final stages (Hu et al., 2024; Huang et al., 2021). Protein glycation is a classical protein-polysaccharide chemical crosslinking process, in which the aldehyde group of a polysaccharide reacts with the amino group of a protein reacts to form conjugates (Hu et al., 2022). Therefore, according to the glycation protocol in our and others' previous work (Hu et al., 2022; Huang et al., 2020; Zhang et al., 2022), the OA and polysaccharides (XG, GG, and KGM) could react to form OPCs.

As shown in Fig. 1A and B, the OA/polysaccharide mixtures were in white fog. After the glycation reaction (90 °C and 1 h), the obtained OPC solutions were still in white fog. It suggested that the glycation reaction did not change the colors of reaction solutions. The obtained freeze-dried solid OPC (solid conjugates) were in white. The pure OA solutions (4 and 10 mg/mL) after room temperature storage showed precipitations in the bottom of the bottles (Figs. 1C and S1). It suggested that the OA was more hydrophobic and easy to aggregate in an aqueous solution (Zheng et al., 2022). These three polysaccharides (anionic XG, nonionic GG, and nonionic KGM) are commonly water-soluble (Hu et al., 2022; Zhang et al., 2022). Therefore, the glycation could increase the solubility of OA in the aqueous solution.

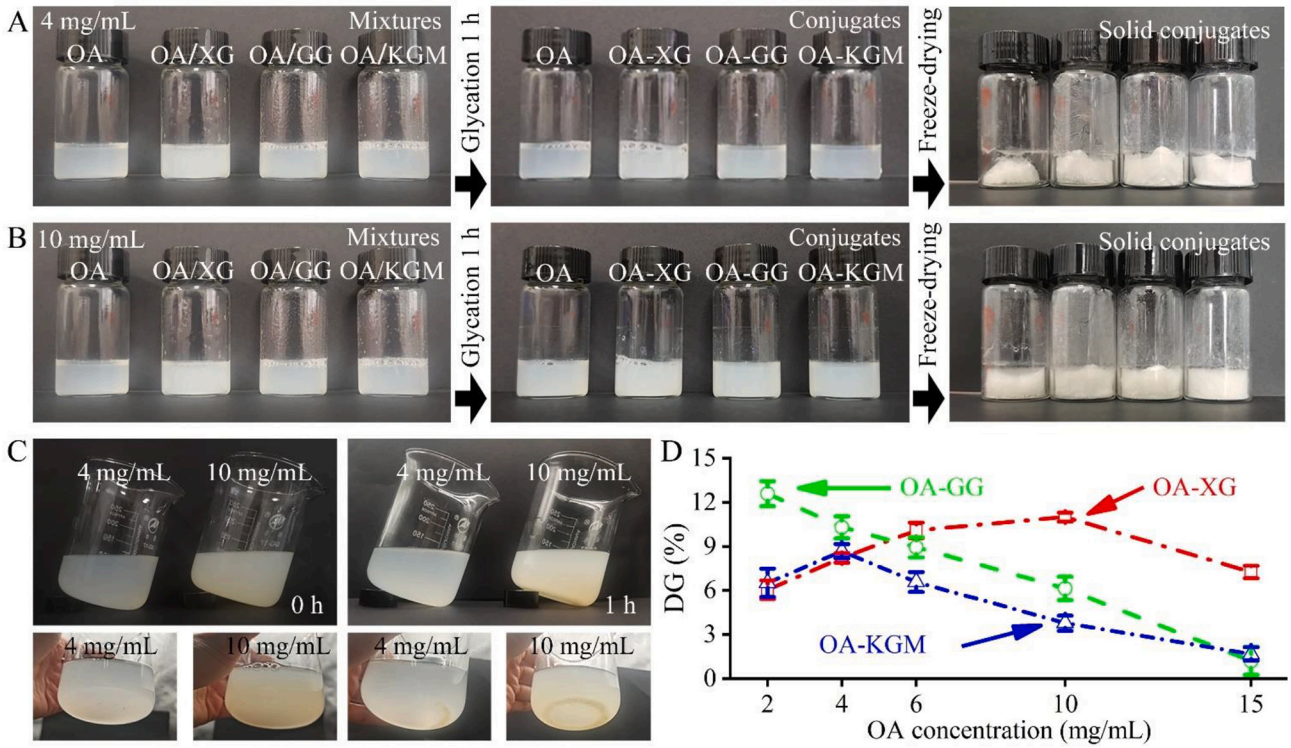

Fig. 1. Preparation and characterization of ovalbumin (OA)-polysaccharide conjugates (OPCs) with a polysaccharide concentration of 2 mg/mL and different OA concentrations. (A–B): OA (A: 4 mg/mL; B: 10 mg/mL) and polysaccharides (XG, xanthan gum; GG, guar gum; KGM, konjac glucomannan) were glycated (90 °C and 1 h) and then the obtained conjugates were freeze-dried to form solid conjugate samples. (C): Storage of OA solutions for different times (0 and 1 h) at room temperature. The upper row showed the solutions in the tilted glass beakers. The lower row showed the bottom of the solutions in the tilted glass beakers. (D): Degree of grafting (DG) of OA with different OA concentrations.

The DG value was used to analyze if the glycation reaction occurred or not (Wen et al., 2020). As shown in Fig. 1D, all the final products showed different DG values from 1.2% to 12.6%, which suggested that OPCs were successfully prepared after the glycation process. The DG values of OA-GG conjugates decreased with the increase of OA concentrations. The steric effect on the glycation reaction was almost the same in the OA concentration range. Therefore, the DG values linearly decreased with the increasing OA concentrations. With the increase of the OA concentrations (Fig. 1D), the DG values of OA-XG and OA-KGM conjugates increased and then decreased. Therefore, the DG values did not linearly decrease with the increasing OA concentrations. These DG change trends were different from that of the fish gelatin-polysaccharide conjugates' DG values (Hu et al., 2022). Therefore, the glycation crosslinking degree was dependent on both the type and concentrations of both proteins and polysaccharides.

3.2. Structural properties of OPCs

The freeze-dried OPCs, OA, and polysaccharides were observed by SEM (Fig. 2A). All the samples showed sheet-like structures. The sheet sizes of OPCs were larger than those of both OA and polysaccharides. They further confirmed that OPCs were successfully prepared after the glycation process. Moreover, these three types of freeze-dried OPCs have different sheet morphologies. It might result from that the three polysaccharides might have different glycation crosslinking behaviors with OA (Fig. 2A).

ATR-FTIR spectrometry was applied to analyze the structural information of OPCs. OA and polysaccharides were treated with the same OPC preparation process and used as controls. As shown in Fig. 2B, OA showed four obvious bands: amide A (3278 cm^{-1}), amide B (2926 cm^{-1}), amide I (1627 cm^{-1} with a shoulder peak of 1650 cm^{-1}), and amide II (1539 cm^{-1}). It also showed weak amide III bands (1239 cm^{-1}). The band peaks were different from the five obvious bands of collagen

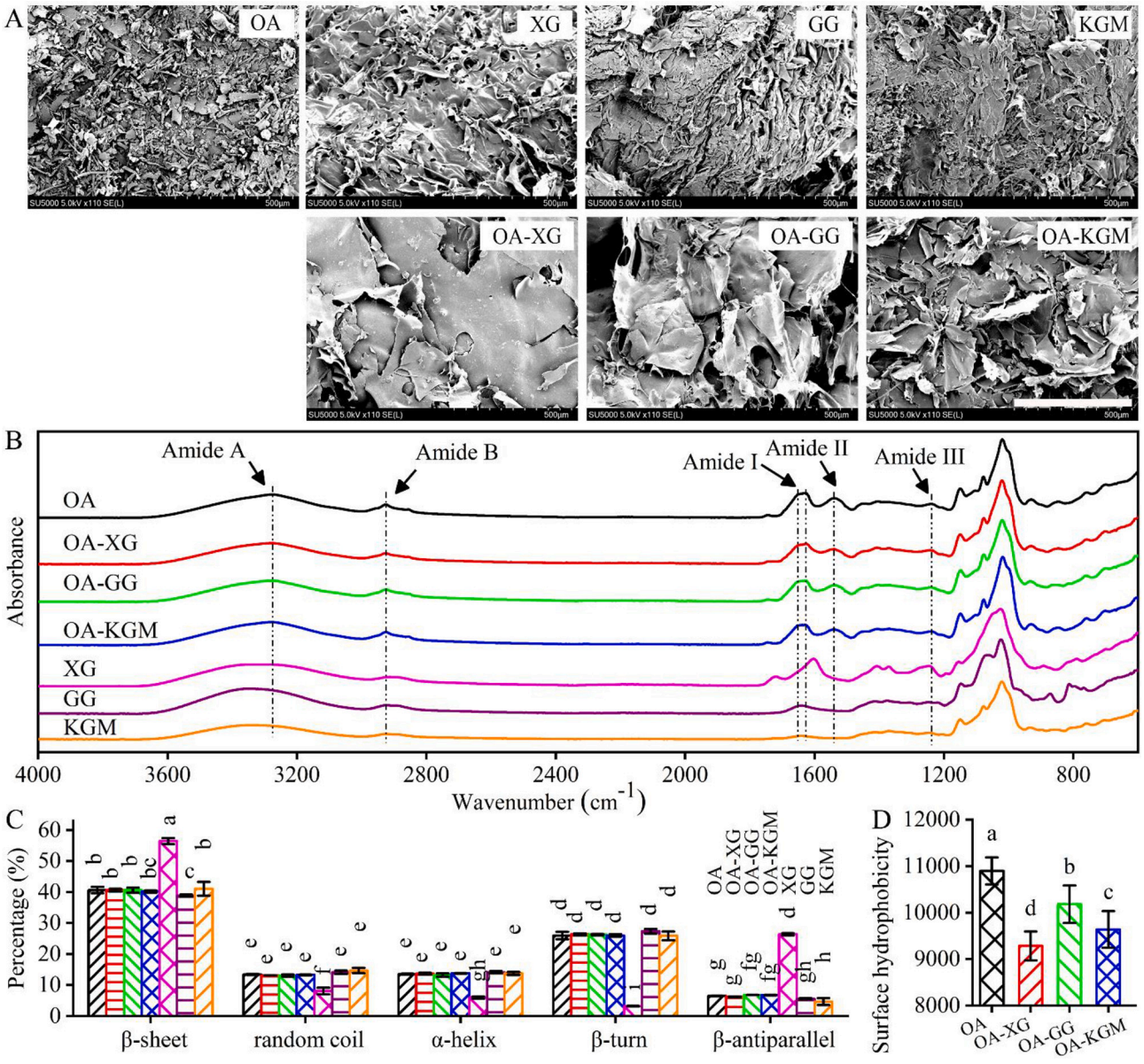

Fig. 2. Structural properties of freeze-dried OPCs with an OA concentration of 4 mg/mL and a polysaccharide concentration of 2 mg/mL. Freeze-dried OA and polysaccharides were used as controls. (A): Scanning electron microscopy. The scale bar indicates 500 μm. (B): Attenuated total reflectance Fourier transform infrared spectra with the wavenumber range of 4000–600 cm^{-1}. (C): Secondary structure percentages. (D): Molecular surface hydrophobicity of OPCs and OA. Different lowercase letters indicate significant differences ($p < 0.05$) in each image.

(Bi et al., 2019). These five band peaks were almost similar to those of the previously reported OA except that no shoulder peak was present in the amide I band (Castanha et al., 2023). Polysaccharides showed different spectra bands to the OA (e.g., no shoulder peaks at the corresponding wavenumber of the polysaccharide band peaks). However, the OPCs showed the same shapes of the five bands to the OA. It suggested that the spectra band intensities of the polysaccharides were significantly weaker than those of OA. Moreover, the glycation with three polysaccharides did not change the spectra bands of OA.

As shown in Figs. 2C and S2, the secondary structure percentages of OPCs were analyzed by peakfitting the ATR-FTIR spectra of the amide I band (1700–1600 cm^{-1}) (Xu et al., 2021). In order to analyze the effect of polysaccharides on the OPCs, the absorption of polysaccharides at 1700–1600 cm^{-1} was also fitted. The comparisons among OA, OPCs, and polysaccharides suggested the glycation with three types of polysaccharides did not change the secondary structure percentages of OA. Previous work suggested OA is in a sphere shape at pH 3 and a polymeric shape at pH 7 (Xu et al., 2020). Therefore, no obvious structural changes of OA were reasonable that the polysaccharides might interact with the side functional groups of the polymeric OA at the preparation pH of 6.1. The secondary structure percentages of OA and OPCs were: β-sheet > β-turn > α-helix ≈ random coil > β-antiparallel.

ANS fluorescent probe method can be applied to analyze the molecular surface hydrophobicity of a protein because ANS can bind with the buried hydrophobic groups of a protein to significantly increase the fluorescence up to 100 times (Munishkina & Fink, 2007). As shown in Fig. 2D, the OPCs had lower molecular surface hydrophobicity values than OA: OA-XG (9284 ± 311) < OA-KGM (9638 ± 393) < OA-GG (10,183 ± 403) < OA (10,897 ± 291). It suggested the OPCs were successfully prepared after the glycation process, which confirmed the conclusion from the DG results (Fig. 1D). Considering OA was more hydrophobic and could be aggregated to form precipitation in water (Fig. 1C) (Zheng et al., 2022), the decrease of the molecular surface hydrophobicity might increase the amphiphilicity of the OA, and might increase the emulsifying properties of the OA.

3.3. Effects of OA preparation concentrations and polysaccharide types on the OPC-stabilized emulsions

As shown in Fig. 3, the fish oil-loaded OPC-stabilized emulsions were prepared with different OA preparation concentrations (4 and 10 mg/mL) and polysaccharide types (XG, GG, and KGM). All the freshly obtained emulsions were in typical milk-white color and were consisted of microscale droplets (Fig. 3A: 0 min; Fig. 3B: 0 min). The OA-stabilized emulsions showed tetramodal distribution for the droplet sizes (Fig. 3C, D, and S3). However, the OPC-stabilized emulsions showed

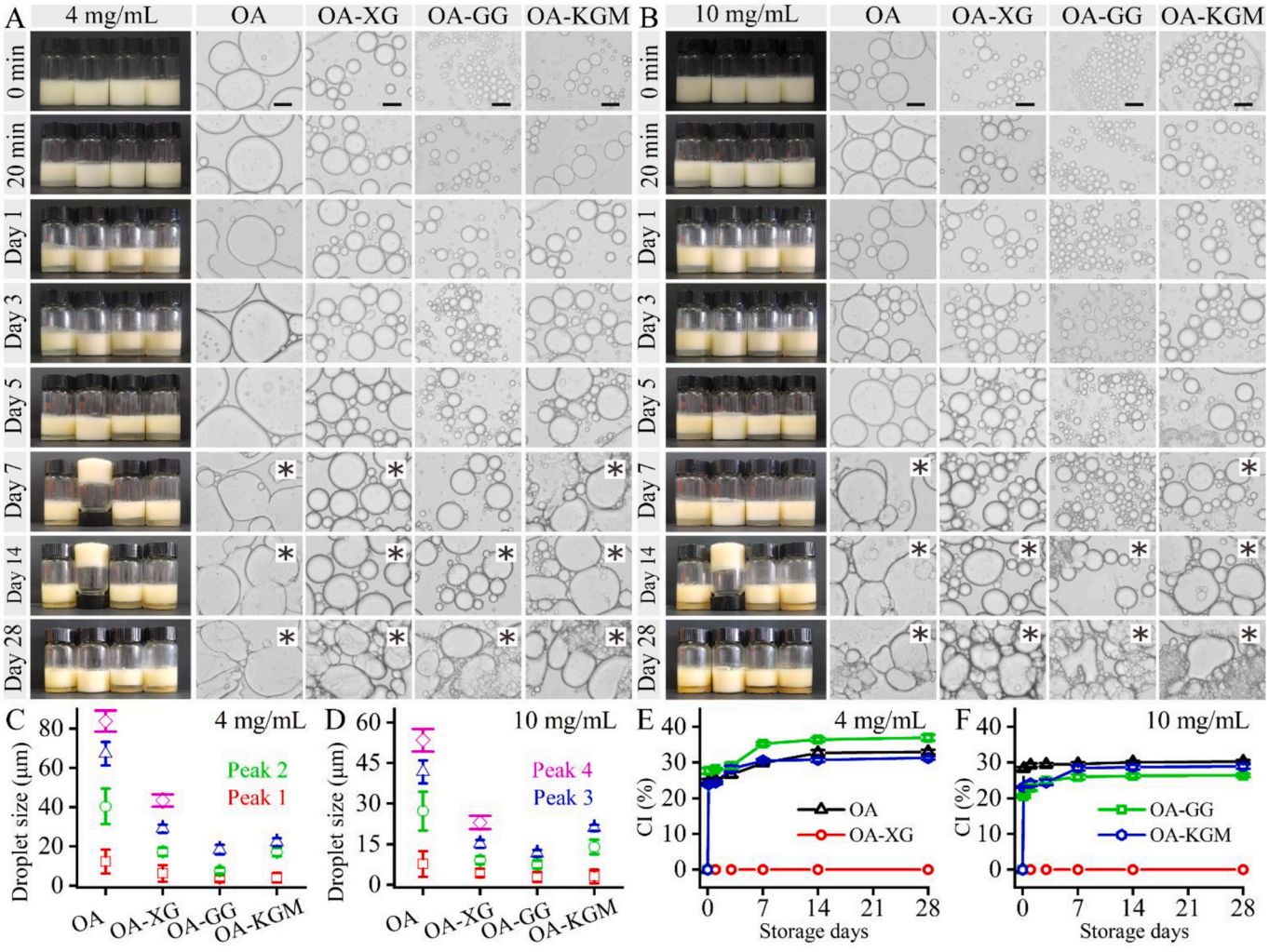

Fig. 3. Stability of the fish oil emulsions stabilized by OPCs with a polysaccharide of 2 mg/mL and different OA concentrations. The OPCs were prepared by a glycation reaction (90 °C and 1 h) with a polysaccharide concentration of 2 mg/mL, an unadjusted glycation pH, and different OA concentrations (4 and 10 mg/mL). The emulsions were stored at room temperature. OA was used as a control. (A–B): Digital camera and optical microscopy images of the emulsions. The scale bars indicate 30 μm. Black asterisks indicate emulsions gels. (C—D): Initial droplet sizes of the emulsions. (E–F): Creaming index (CI) values of the emulsions.

trimodal distribution for the droplet sizes. The glycation by three types of polysaccharides significantly decreased the droplet sizes of the emulsions. Moreover, the droplet sizes were dependent on the applied polysaccharides: OA > OA-XG > OA-KGM > OA-GG. In addition, the droplet sizes at high OA concentration (10 mg/mL) were larger than those at low OA concentration (4 mg/mL). This trend was accorded with those of the emulsions stabilized by proteins such as bovine bone gelatin nanoparticles (Gong et al., 2024) and tilapia scale gelatin (Peng et al., 2022). Therefore, the initial droplet sizes were dependent on the polysaccharide types and the OA preparation concentrations.

The storage stability of the fish oil-loaded emulsions at room temperature was analyzed such as liquid-gel transition, creaming stability, and droplet stability (Fig. 3). The emulsions changed from liquid to gel at day 7 or 14 (Indicated by black asterisks in Fig. 3). The liquid-gel transition time was mainly dependent on the polysaccharide types. It was dependent on the OA preparation concentrations (OA-XG: day 7 for 4 mg/mL and day 14 for 10 mg/mL) or not (OA and OA-KGM: day 7; OA-GG: day 14). The creaming stability was mainly dependent on the applied polysaccharides and minorly dependent on the OA preparation concentrations (Fig. 3E and F). KGM glycation slightly decreased the emulsion CI values. GG glycation increased or decreased the emulsion CI values at low (4 mg/mL) or high (10 mg/mL) OA preparation concentrations, respectively. In particular, XG glycation induced no obvious creaming during the 28-day storage. As shown in the optical microscopy images of Fig. 3, all the droplet sizes increased with time due to droplet coalescence (Li & Van der Meeren, 2022). Moreover, the droplet sizes of the OPC-stabilized emulsions were significantly less than those of the OA-stabilized emulsions, which confirmed that polysaccharide glycation could decrease the emulsion droplet sizes. All these results demonstrated the emulsion stability was mainly dependent on the polysaccharide types and minorly dependent on the OA preparation concentrations.

The emulsion CI value is generally positively correlated with the droplet move rate (V_{stokes}). Stokes' Law was used to describe the affecting factors for the droplet move rate (McClements & Jafari, 2018; Yang, Yang, et al., 2022):

$$V_{stokes} = -\frac{2gr^2(\rho_2 - \rho_1)}{9\eta_1} \quad (1)$$

where g, r, ρ_2, ρ_1, *and* η_1 are the gravity acceleration, initial droplet radius, droplet density, water phase density, and water phase viscosity, respectively. According to the Stokes' Law (Eq. 1), the CI value is positively correlated with the initial droplet radius. Among the OA and OPCs (Fig. 3), the OA-GG conjugate induced the lowest initial droplet sizes (Fig. 3C and D), whereas it did not induce the lowest CI values (Fig. 3E and F). It suggested that the initial droplet size might not be the major factor affecting the creaming stability of the emulsions stabilized by different OA preparation concentrations and polysaccharide types according to Stokes' Law (Eq. 1). In addition, the DG values (Fig. 1D) did not show obvious relationships to the initial droplet sizes (Figs. 3D) and the CI values (Figs. 3F). Therefore, the droplet sizes and creaming stability of the emulsions was not directly dependent on the DG values of OPCs with different polysaccharide types. However, it did not mean that the changes in DG of the same complex have no effect on the droplet size and stability of the emulsion.

3.4. Effect of GG: OA mass ratio on the OPC-stabilized emulsions

Among the three types of OPCs, OA-GG conjugate induced the smallest initial droplet sizes of the fish oil emulsions (Fig. 3C and D). Therefore, the OA-GG conjugates (Fig. S4) were prepared using a glycation reaction with different GG: OA mass ratios (1:5, 2:5, 3:5, 4:5, and 1:1) to analyze their effect on the preparation and stability of the OPC-stabilized emulsions. Both the OA/GG mixtures and OA-GG conjugates solutions were in white fog. Therefore, the glycation reaction with different GG: OA mass ratios did not change the colors of reaction solutions. It was consistent with the unchanged color of OPCs at different OA concentrations (Fig. 1A and B) after the glycation reaction.

The OPCs with different GG: OA mass ratios were used to prepare fish oil-loaded emulsions (Fig. 4). All the freshly obtained emulsions were in typical milk-white color and consisted of microscale droplets (Fig. 4A: 0 h). The OPC-stabilized emulsions showed bimodal (2:5 and 3:5) or trimodal (1:5, 4:5, and 1:1) distribution for the droplet sizes (Figs. 4C and S5). Moreover, the droplet sizes were dependent on the GG: OA mass ratio: 1:1 > 4:5 ≈ 1:5 > 2:5 ≈ 3:5. In addition, the viscosity was dependent on the GG: OA mass ratio (Fig. 4B: 0 h). The emulsion at a GG: OA mass ratio of 1:1 showed higher viscosity than that at a GG: OA mass ratio of 3:5. Therefore, the glycation with higher GG amounts induced the higher emulsion viscosity.

The storage stability of the fish oil-loaded emulsions at room temperature was analyzed such as liquid-gel transition, viscosity change, creaming stability, and droplet stability (Fig. 4). The GG: OA mass ratio of 1:1 induced the liquid-gel transition time of 1 day and others induced the time of 7 days. Therefore, the liquid-gel transition time was dependent on the GG: OA mass ratios. As shown in Fig. 4B, the emulsion viscosity increased with time. It confirmed the transition of the emulsions from liquid to gel. The creaming stability increased with the increase of GG: OA mass ratios (Fig. 4A and D). Moreover, the emulsions showed no obvious creaming at the GG: OA mass ratios of ≥3:5. As shown in the optical microscopy images of Fig. 4A, all the droplet sizes increased with time due to droplet coalescence (Li & Van der Meeren, 2022). Moreover, higher (≥2:5) GG: OA mass ratios induced stronger droplet stabilization ability than lower (1:5) GG: OA mass ratios (Fig. 4A: Day 14 and 28). It suggested that polysaccharide glycation could increase the emulsion droplet stability, which might be due to the induction of polysaccharides. All these results demonstrated the stability of the emulsions stabilized by OPCs was dependent on the GG: OA mass ratios.

For the emulsions stabilized by OA-GG conjugates with different GG: OA mass ratios (Fig. 4), the emulsion CI values were not positively correlated with the initial droplet sizes (Fig. 4A, C, and D), which was not consistent with the positive relationship between the CI value and initial droplet radius in the Stokes' Law (Eq. 1). It was also consistent with the results in Fig. 3. According to the Stokes' Law (Eq. 1), we could conclude that the initial droplet size was not the major factor to affect the creaming stability of the emulsions stabilized by OPCs with different polysaccharide: OA mass ratios.

The DG values of OA-GG conjugates were increased and then decreased with the increasing GG: OA mass ratios (Fig. 4E). The results confirmed the successful preparation of OA-GG conjugates with different GG: OA mass ratios. However, the DG values did not show obvious relationships to the initial droplet sizes (Fig. 4C) and the CI values (Fig. 4D). Therefore, the initial droplet sizes and creaming stability of the emulsions were not directly dependent on the DG values of OA-GG conjugates. However, it did not mean that the changes in DG of the same complex have no effect on the droplet size and stability of the emulsion.

3.5. Effect of glycation pH on the OPC-stabilized emulsions

Among the three types of OPCs, OA-XG conjugate induced no obvious creaming of the fish oil emulsions during the 28-day storage at room temperature (Fig. 3E and F). Therefore, the OA-XG conjugates (Fig. S6) were prepared at different glycation pH (6.1 of unadjusted pH, 3.0, 5.0, 7.0, 9.0, and 11.0) to analyze their effect on the preparation and stability of the OPC-stabilized emulsions. Both the OA/XG mixtures and OA-XG conjugates solutions were in white fog (Fig. S6). Therefore, the glycation reaction with different pH did not change the colors of the reaction solutions. It was consistent with the unchanged color of OPCs at different OA concentrations (Fig. 1A and B) and GG: OA mass ratios (Fig. S4) after the glycation reaction.

The OPCs with different glycation pH were used to prepare fish oil-

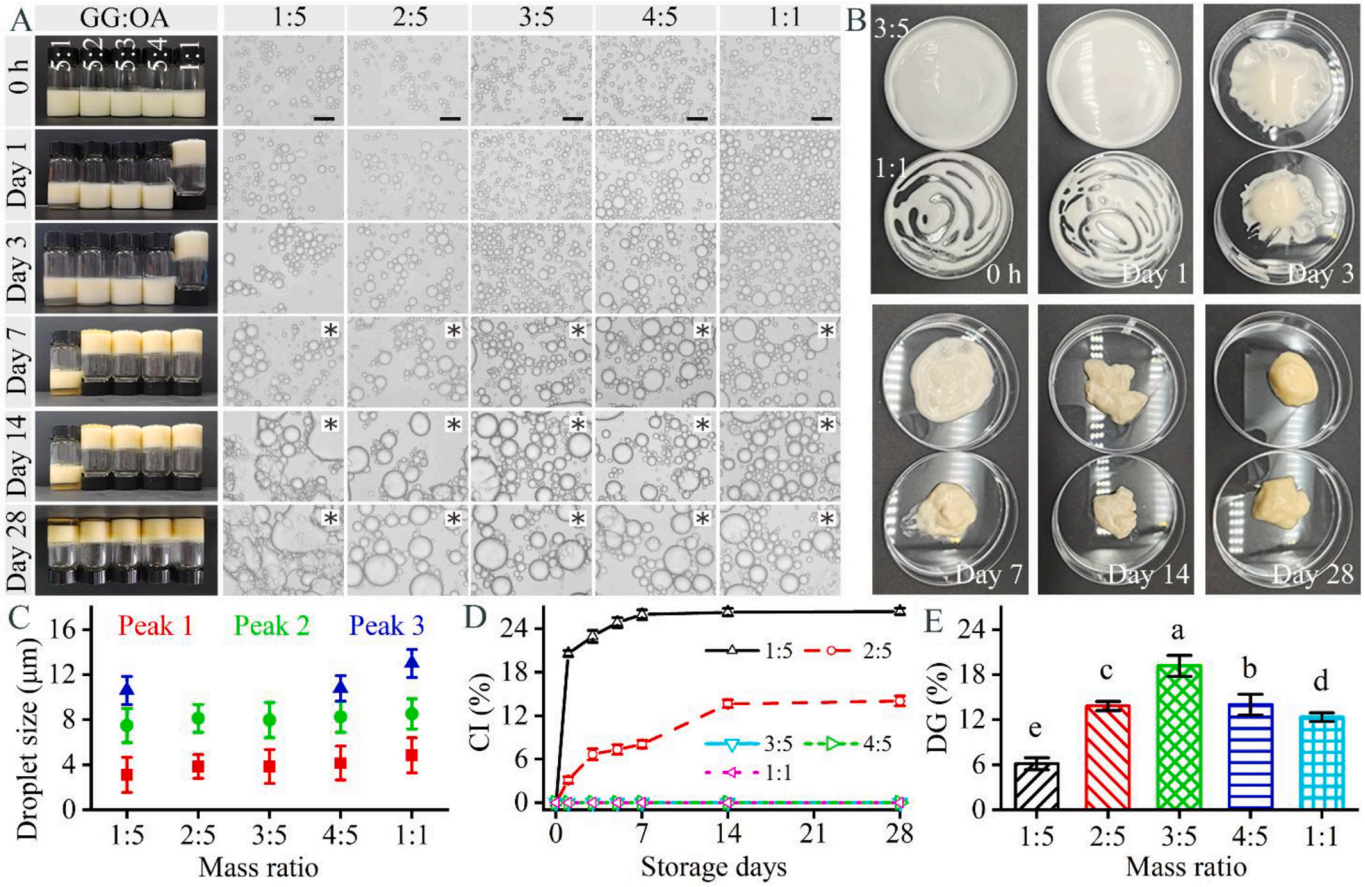

Fig. 4. Stability of the fish oil emulsions stabilized by OA-GG conjugates with different GG: OA mass ratios. The OA-GG conjugates were prepared by a glycation reaction (90 °C and 1 h) with an OA concentration of 10 mg/mL, an unadjusted glycation pH, and different GG: OA mass ratios (1:5, 2:5, 3:5, 4:5, and 1:1). The emulsions were stored at room temperature. (A): Digital camera and optical microscopy images. The scale bars indicate 30 μm. Black asterisks indicate emulsions gels. (B): At different storage times, the emulsions stabilized by OPCs with the GG: OA mass ratios of 3:5 and 1:1 in the glass vials were put in plastic Petri dishes with 90 mm in diameter. (C): Initial droplet sizes of the emulsions. (D): CI values of the emulsions. (E): DG of OA with different GG: OA mass ratios. Different lowercase letters indicate significant differences ($p < 0.05$).

loaded emulsions (Fig. 5). All the freshly obtained emulsions were in typical milk-white color and consisted of microscale droplets (Fig. 5A: 0 h). Droplet coalescence occurred with the glycation pH of 3.0, which suggested that pH 3.0 was not an appropriate pH to prepare OPCs for emulsion preparation. The OPC-stabilized emulsions showed trimodal distribution for the droplet sizes (Fig. 5B and S7). Moreover, the droplet sizes were dependent on the glycation pH. The glycation pH of 5.0, 6.1, and 9.0 induced relatively smaller droplet sizes than the glycation pH of 7.0 and 11.0 (Figs. 5B and S7). Therefore, weak acidic and basic pH might be the appropriate pH to prepare OPCs for the stabilization of fish oil emulsions with small droplet sizes.

The storage stability of the fish oil-loaded emulsions at room temperature was analyzed such as liquid-gel transition, creaming stability, and droplet stability (Fig. 5). The emulsions stabilized by OPCs with a glycation pH of 3.0 showed obvious droplet disruption during the whole storage. Therefore, emulsion could not be formed at pH 3.0 according to the optical microscopy images. All the emulsions showed different liquid-gel transition times (pH 5.0, 6.1, and 11.0: 7 days; pH 7.0 and 9.0: 14 days). Therefore, the liquid-gel transition time was dependent on the glycation pH. The creaming stability was also dependent on the glycation pH (Fig. 5A and D). Moreover, the emulsions showed no obvious creaming at the glycation pH of 5.0 and 6.1. As shown in the optical microscopy images of Fig. 5A, all the droplet sizes increased with time due to droplet coalescence (Li & Van der Meeren, 2022). pH 11.0 induced the droplet disruption at day 5. All the other emulsion droplets were disrupted on day 28. These results suggested that glycation pH had an obvious effect on the emulsion droplet stability.

For the emulsions stabilized by OA-XG conjugates with different glycation pH (Fig. 5), the emulsion CI values were not positively correlated with the initial droplet sizes (Fig. 5A, B, and C), which was not consistent with the relationship between the CI value and initial droplet radius in the Stokes' Law (Eq. 1). It was consistent with the results in the Figs. 3 and 4. According to Stokes' Law (Eq. 1), we could conclude that the initial droplet size was not the major factor affecting the creaming stability of the emulsions stabilized by OPCs with different glycation pH.

The DG values of OA-XG conjugates were dependent on the glycation pH (Fig. 5D): pH 11.0 > pH 5.0 > pH 6.1 > pH 3.0 > pH 7.0 > pH 9.0. The results confirmed the successful preparation of OA-XG conjugates with different glycation pH. However, the DG values did not show obvious relationships to the initial droplet sizes (Fig. 5B) and the CI values (Fig. 5C). Therefore, the initial droplet sizes and creaming stability of the emulsions were not dependent on the glycation pH of OA-GG conjugates.

4. Conclusions

This work studied the effect of glycation with three polysaccharides on the structural and emulsifying properties of OA. The glycation with three polysaccharides showed different effects on the OA-polysaccharide grafting to form OPCs and their application to stabilize the fish oil-loaded emulsions. This work provided useful information to

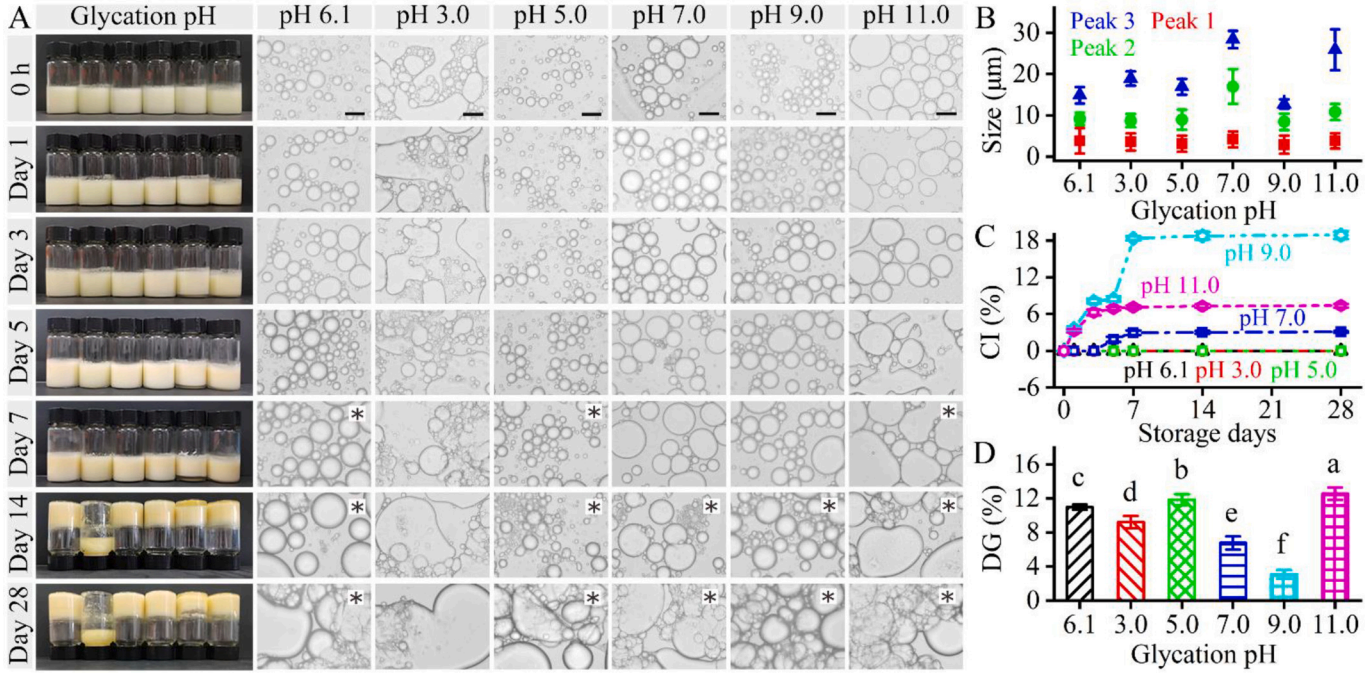

Fig. 5. Effect of glycation pH on the storage stability of the fish oil emulsions stabilized by OA-XG conjugates with different glycation pH. The OA-XG conjugate was prepared by a glycation reaction (90 °C and 1 h) with an OA concentration of 10 mg/mL, an XG concentration of 2 mg/mL, and different glycation pH (6.1 of unadjusted pH, 3.0, 5.0, 7.0, 9.0, and 11.0). The emulsions were stored at room temperature. (A): Digital camera and optical microscopy images. The scale bars indicate 30 μm. Black asterisks indicate emulsions gels. (B): Initial droplet sizes of the emulsions. (C): Creaming indexes of the emulsions. (D): DG of OA with different glycation pH. Different lowercase letters indicate significant differences ($p < 0.05$).

understand the effect of molecular modification on the structural and functional properties of a protein. It also provided promising OA-polysaccharide conjugates for emulsifier development in the field of food science.

Further studies are still required for the development and application of OPCs in the future. First, the obtained OPCs might have impurities such as OA and polysaccharides. Almost no separation step was applied to purify protein-polysaccharide conjugates after the glycation step in the previous related works. However, further work is interesting to explore purification methods to obtain pure OPCs for emulsion stabilization. Second, though polysaccharide glycation of a protein is a mature method to prepare protein-polysaccharide conjugates, comprehensive characterization analyses of the OPCs are useful to understand their structure-function relationship using additional characterization techniques such as gel permeation chromatography, circular dichroism, differential scanning calorimetry, and three-phase contact angle measurement. The results will further ascertain whether binding occurs between polysaccharides and proteins, as well as the type of binding. Third, comprehensive characterization analyses of the emulsion stabilization are required using additional characterization techniques such as laser particle size analyzer, zeta potential analyzer, and rheometer. The results would be useful to understand the stabilization process and mechanism of the emulsions. Finally, it is also interesting to explore the effect of glycation with more anionic polysaccharides on the structural and functional properties of OA.

CRediT authorship contribution statement

Yaxue Hu: Writing – original draft, Investigation, Formal analysis, Data curation. **Qiqi Bian:** Investigation. **Lijia Chen:** Investigation. **Xichang Wang:** Resources. **Jian Zhong:** Writing – review & editing, Funding acquisition, Formal analysis, Data curation, Conceptualization.

Declaration of competing interest

The authors declare that they have no known competing financial interests or personal relationships that could have appeared to influence the work reported in this paper.

Data availability

Data will be made available on request.

Acknowledgments

This research has been supported by research grants from the National Natural Science Foundation of China (No. 32272338) and Shanghai Municipal Three Year Action Plan for Strengthening the Construction of Public Health System (2023-2025) Discipline Leader Project (GW*V*I-11.2-XD19).

Appendix A. Supplementary data

Supplementary data to this article can be found online at https://doi.org/10.1016/j.fochx.2024.101632.

References

Amiratashani, F., Yarmand, M. S., Kiani, H., Askari, G., Naeini, K. K., & Parandi, E. (2024). Comprehensive structural and functional characterization of a new protein-polysaccharide conjugate between grass pea protein (Lathyrus sativus) and xanthan gum produced by wet heating. *International Journal of Biological Macromolecules, 254*, Article 127283. https://doi.org/10.1016/j.ijbiomac.2023.127283

Bi, C., Li, X., Xin, Q., Han, W., Shi, C., Guo, R., Shi, W., Qiao, R., Wang, X., & Zhong, J. (2019). Effect of extraction methods on the preparation of electrospun/electrosprayed microstructures of tilapia skin collagen. *Journal of Bioscience and Bioengineering, 128*, 234–240. https://doi.org/10.1016/j.jbiosc.2019.02.004

Castanha, E., Kavalek, R. L., Hoff, R. B., Dacoreggio, M. V., Jesus, B. A. P. D., MagalhÃEs, M. D. L. B., … Kempka, A. P. (2023). Non-covalent binding of phenolic compounds from leaves of Campomanesia xanthocarpa (Mart.) O. Berg with ovalbumin: Effect on protein structure, amino acids involved in the complexation

and antioxidant activity. *Food chemistry. Advances, 2*, Article 100303. https://doi.org/10.1016/j.focha.2023.100303
Chen, Q., Dong, L., Li, Y., Liu, Y., Xia, Q., Sang, S., Wu, Z., Xiao, J., Liu, L., & Liu, L. (2024). Research advance of non-thermal processing technologies on ovalbumin properties: The gelation, foaming, emulsification, allergenicity, immunoregulation and its delivery system application. *Critical Reviews in Food Science and Nutrition, 1-22*. https://doi.org/10.1080/10408398.2023.2179969
Feng, S., Guo, Y., Liu, F., Li, Z., Chen, K., Handa, A., & Zhang, Y. (2023). The impacts of complexation and glycated conjugation on the performance of soy protein isolate-gum Arabic composites at the o/w interface for emulsion-based delivery systems. *Food Hydrocolloids, 135*, Article 108168. https://doi.org/10.1016/j.foodhyd.2022.108168
Galazka, V. B., Dickinson, E., & Ledward, D. A. (2000). Emulsifying properties of ovalbumin in mixtures with sulphated polysaccharides: Effects of pH, ionic strength, heat and high-pressure treatment. *Journal of the Science of Food and Agriculture, 80*, 1219–1229. https://doi.org/10.1002/1097-0010(200006)80:8<1219::AID-JSFA626>3.0.CO;2-W
Gong, H., Zi, Y., Kan, G., Li, L., Shi, C., Wang, X., & Zhong, J. (2024). Preparation of food-grade EDC/NHS-crosslinked gelatin nanoparticles and their application for Pickering emulsion stabilization. *Food Chemistry, 436*, Article 137700. https://doi.org/10.1016/j.foodchem.2023.137700
Hu, Y., Bian, Q., Zi, Y., Shi, C., Peng, J., Zheng, Y., Wang, X., & Zhong, J. (2024). Molecular modification of low-dissolution soy protein isolates by anionic xanthan gum, neutral guar gum, or neutral konjac glucomannan to improve the protein dissolution and stabilize fish oil emulsion. *International Journal of Biological Macromolecules, 267*, Article 131521. https://doi.org/10.1016/j.ijbiomac.2024.131521
Hu, Y., Zhang, Y., Xu, J., Zi, Y., Peng, J., Zheng, Y., Wang, X., & Zhong, J. (2022). Fish gelatin-polysaccharide Maillard products for fish oil-loaded emulsion stabilization: Effects of polysaccharide type, reaction time, and reaction pH. *LWT, 172*, Article 114220. https://doi.org/10.1016/j.lwt.2022.114220
Huang, T., Tu, Z., Shangguan, X., Wang, H., Zhang, L., & Bansal, N. (2021). Characteristics of fish gelatin-anionic polysaccharide complexes and their applications in yoghurt: Rheology and tribology. *Food Chemistry, 343*, Article 128413. https://doi.org/10.1016/j.foodchem.2020.128413
Huang, T., Tu, Z., Zou, Z., Shangguan, X., Wang, H., & Bansal, N. (2020). Glycosylated fish gelatin emulsion: Rheological, tribological properties and its application as model coffee creamers. *Food Hydrocolloids, 102*, Article 105552. https://doi.org/10.1016/j.foodhyd.2019.105552
Lan, Y.-C., & Lai, L.-S. (2023). Pasting and rheological properties of water caltrop starch as affected by the addition of konjac glucomannan, guar gum and xanthan gum. *Food Hydrocolloids, 136*, Article 108245. https://doi.org/10.1016/j.foodhyd.2022.108245
Li, H., & Van der Meeren, P. (2022). Sequential adsorption of whey proteins and low methoxy pectin at the oil-water interface: An interfacial rheology study. *Food Hydrocolloids, 128*, Article 107570. https://doi.org/10.1016/j.foodhyd.2022.107570
Li, K.-Y., Zhang, X.-R., Huang, G.-Q., Teng, J., Guo, L.-P., Li, X.-D., & Xiao, J.-X. (2022). Complexation between ovalbumin and gum Arabic in high total biopolymer concentrations and the emulsifying ability of the complexes. *Colloids and Surfaces A: Physicochemical and Engineering Aspects, 642*, Article 128624. https://doi.org/10.1016/j.colsurfa.2022.128624
Li, R., Xue, H., Gao, B., Liu, H., Han, T., Hu, X., Tu, Y., & Zhao, Y. (2022). Physicochemical properties and digestibility of thermally induced ovalbumin–oil emulsion gels: Effect of interfacial film type and oil droplets size. *Food Hydrocolloids, 131*, Article 107747. https://doi.org/10.1016/j.foodhyd.2022.107747
Li, S., Huang, Y., An, F., Huang, Q., Geng, F., & Ma, M. (2019). Hydroxyl radical-induced early stage oxidation improves the foaming and emulsifying properties of ovalbumin. *Poultry Science, 98*, 1047–1054. https://doi.org/10.3382/ps/pey370
Li, Y.-X., Wang, N.-N., Yan, Q.-J., Hua, X.-H., Liu, Y., & Jiang, Z.-Q. (2022). A novel neutral thermophilic β-mannanase from *Malbranchea cinnamomea* for controllable production of partially hydrolyzed konjac powder. *Applied Microbiology and Biotechnology, 106*, 1919–1932. https://doi.org/10.1007/s00253-022-11832-2
Liu, L., Li, Y., Dai, X., Zhu, Y., Hao, W., & Yang, X. (2020). Effects of synergistic modification with enzymatic hydrolysis and phosphorylation on functional and structural properties of ovalbumin. *Journal of Food Processing and Preservation, 44*, Article e14934. https://doi.org/10.1111/jfpp.14934
McClements, D. J., & Jafari, S. M. (2018). Improving emulsion formation, stability and performance using mixed emulsifiers: A review. *Advances in Colloid and Interface Science, 251*, 55–79. https://doi.org/10.1016/j.cis.2017.12.001
Mine, Y., Noutomi, T., & Haga, N. (1991). Emulsifying and structural properties of ovalbumin. *Journal of Agricultural and Food Chemistry, 39*, 443–446. https://doi.org/10.1021/jf00003a003
Munishkina, L. A., & Fink, A. L. (2007). Fluorescence as a method to reveal structures and membrane-interactions of amyloidogenic proteins. *Biochimica et Biophysica Acta (BBA) -Biomembranes, 1768*, 1862–1885. https://doi.org/10.1016/j.bbamem.2007.03.015
Nsengiyumva, E. M., Heitz, M. P., & Alexandridis, P. (2024). Salt and temperature effects on xanthan gum polysaccharide in aqueous solutions. *International Journal of Molecular Sciences, 25*, 490. https://doi.org/10.3390/ijms25010490
Peng, J., Zi, Y., Xu, J., Zheng, Y., Huang, S., Hu, Y., Liu, B., Wang, X., & Zhong, J. (2022). Effect of extraction methods on the properties of tilapia scale gelatins. *International Journal of Biological Macromolecules, 221*, 1150–1160. https://doi.org/10.1016/j.ijbiomac.2022.09.094
Rostamabadi, H., Chaudhary, V., Chhikara, N., Sharma, N., Nowacka, M., Demirkesen, I., … Falsafi, S. R. (2023). Ovalbumin, an outstanding food hydrocolloid: Applications, technofunctional attributes, and nutritional facts, A systematic review. *Food Hydrocolloids, 139*, Article 108514. https://doi.org/10.1016/j.foodhyd.2023.108514
Sharma, G., Sharma, S., Kumar, A., Al-Muhtaseb, A. A. H., Naushad, M., Ghfar, A. A., … Stadler, F. J. (2018). Guar gum and its composites as potential materials for diverse applications: A review. *Carbohydrate Polymers, 199*, 534–545. https://doi.org/10.1016/j.carbpol.2018.07.053
Tang, S., Yu, J., Lu, L., Fu, X., & Cai, Z. (2019). Interfacial and enhanced emulsifying behavior of phosphorylated ovalbumin. *International Journal of Biological Macromolecules, 131*, 293–300. https://doi.org/10.1016/j.ijbiomac.2019.03.076
Wen, C., Zhang, J., Qin, W., Gu, J., Zhang, H., Duan, Y., & Ma, H. (2020). Structure and functional properties of soy protein isolate-lentinan conjugates obtained in Maillard reaction by slit divergent ultrasonic assisted wet heating and the stability of oil-in-water emulsions. *Food Chemistry, 331*, Article 127374. https://doi.org/10.1016/j.foodchem.2020.127374
Wen, H., Ning, Z., Li, J., Guan, Y., Zhang, B., Shang, X., Liu, X., Du, Z., Liu, J., & Zhang, T. (2022). Stability of oil-in-water emulsions improved by ovalbumin-procyanidins mixture: A promising substrate with emulsifying and antioxidant activity. *Colloids and Surfaces B: Biointerfaces, 215*, Article 112473. https://doi.org/10.1016/j.colsurfb.2022.112473
Xiao, N., He, W., Zhao, Y., Yao, Y., Xu, M., Du, H., Wu, N., & Tu, Y. (2021). Effect of pH and xanthan gum on emulsifying property of ovalbumin stabilized oil-in water emulsions. *LWT, 147*, Article 111621. https://doi.org/10.1016/j.lwt.2021.111621
Xu, J., Yang, L., Nie, Y., Yang, M., Wu, W., Wang, Z., Wang, X., & Zhong, J. (2022). Effect of transglutaminase crosslinking on the structural, physicochemical, functional, and emulsion stabilization properties of three types of gelatins. *LWT, 163*, Article 113543. https://doi.org/10.1016/j.lwt.2022.113543
Xu, J., Zhang, T., Zhang, Y., Yang, L., Nie, Y., Tao, N., Wang, X., & Zhong, J. (2021). Silver carp scale gelatins for the stabilization of fish oil-loaded emulsions. *International Journal of Biological Macromolecules, 186*, 145–154. https://doi.org/10.1016/j.ijbiomac.2021.07.043
Xu, Y.-T., Wang, Y.-H., Chen, F.-P., & Tang, C.-H. (2020). Whether ovalbumin performs as a particulate or polymeric emulsifier is largely determined by pH. *Food Hydrocolloids, 103*, Article 105694. https://doi.org/10.1016/j.foodhyd.2020.105694
Yang, L., Yang, M., Xu, J., Nie, Y., Wu, W., Zhang, T., Wang, X., & Zhong, J. (2022). Structural and emulsion stabilization comparison of four gelatins from two freshwater and two marine fish skins. *Food Chemistry, 371*, Article 131129. https://doi.org/10.1016/j.foodchem.2021.131129
Yang, Q., Wang, Y., Yang, M., Liu, X., Lyu, S., Liu, B., Liu, J., & Zhang, T. (2022). Effect of glycation degree on the structure and digestion properties of ovalbumin: A study of amino acids and peptides release after in vitro gastrointestinal simulated digestion. *Food Chemistry, 373*, Article 131331. https://doi.org/10.1016/j.foodchem.2021.131331
Yang, X., Li, A., Li, D., Li, X., Li, P., Sun, L., & Guo, Y. (2020). Improved physical properties of konjac glucomannan gels by co-incubating composite konjac glucomannan/xanthan systems under alkaline conditions. *Food Hydrocolloids, 106*, Article 105870. https://doi.org/10.1016/j.foodhyd.2020.105870
Yang, X., Li, A., Li, X., Sun, L., & Guo, Y. (2020). An overview of classifications, properties of food polysaccharides and their links to applications in improving food textures. *Trends in Food Science & Technology, 102*, 1–15. https://doi.org/10.1016/j.tifs.2020.05.020
Zeng, Q., Zeng, W., Jin, Y., & Sheng, L. (2022). Construction and evaluation of ovalbumin-pullulan nanogels as a potential delivery carrier for curcumin. *Food Chemistry, 367*, Article 130716. https://doi.org/10.1016/j.foodchem.2021.130716
Zhang, Q., Zhou, Y., Yue, W., Qin, W., Dong, H., & Vasanthan, T. (2021). Nanostructures of protein-polysaccharide complexes or conjugates for encapsulation of bioactive compounds. *Trends in Food Science & Technology, 109*, 169–196. https://doi.org/10.1016/j.tifs.2021.01.026
Zhang, Y., Xu, J., Zhang, T., Tao, L., Nie, Y., Wang, X., & Zhong, J. (2022). Effect of carbon numbers and structures of monosaccharides on the glycosylation and emulsion stabilization ability of gelatin. *Food Chemistry, 389*, Article 133128. https://doi.org/10.1016/j.foodchem.2022.133128
Zheng, Y., Chang, Y., Luo, B., Teng, H., & Chen, L. (2022). Molecular structure modification of ovalbumin through controlled glycosylation with dextran for its emulsibility improvement. *International Journal of Biological Macromolecules, 194*, 1–8. https://doi.org/10.1016/j.ijbiomac.2021.11.130